A 406-year non-growing season precipitation reconstruction in the southeastern Tibetan Plateau

Maierdang Keyimu[1], Zongshan Li[1]*, Bojie Fu[1], Guohua Liu[1], Weiliang Chen[1], Zexin Fan[2], Keyan Fang[3], Xiuchen Wu[4], Xiaochun Wang[5]

[1]State Key Laboratory of Urban and Regional Ecology, Research Center for Eco-Environmental Sciences, Chinese Academy of Sciences, Beijing 100085, China

[2]Xishuangbanna Tropical Botanical Garden, Chinese Academy of Sciences, Mengla 666303, China

[3]Key Laboratory of Humid Subtropical Eco-Geographical Process (Ministry of Education), College of Geographical Sciences, Fujian Normal University, Fuzhou 350007, China

[4]State Key Laboratory of Earth Surface Processes and Resource Ecology, Beijing Normal University, Beijing 100875, China

[5]College of Forestry, Northeast Forestry University, Harbin 150040, China

Correspondence to: Zongshan Li (zsli_st@rcees.ac.cn)

Abstract. Trees record climatic conditions during their growth, and tree rings serve as proxy to reveal the features of the historical climate of a region. In this study, we collected tree-ring cores of forest hemlock (*Tsuga forrestii*) from the northwestern Yunnan area of the southeastern Tibetan Plateau (SETP), and created a residual tree-ring width (TRW) chronology. An analysis of the relationship between tree growth and climate revealed that precipitation during the non-growing season (NGS) (from November of the previous year to February of the current year) was the most important constraining factor on the radial tree growth of forest hemlock in this region. In addition, the influence of NGS precipitation on radial tree growth was relatively uniform over time (1956–2005). Accordingly, we reconstructed the NGS precipitation over the period spanning from A.D. 1600–2005. The reconstruction accounted for 28.5% of the actual variance during the common period 1956–2005. Based on the reconstruction, NGS was extremely dry during the years A.D. 1656, 1670, 1694, 1703, 1736, 1897, 1907, 1943, 1969, 1982, and 1999. In contrast, the NGS was extremely wet during the years A.D. 1627, 1638, 1654, 1832, 1834–1835, and 1992. Similar variations of the NGS precipitation reconstruction series and Palmer Drought Severity Index (PDSI) reconstructions of early growing season from surrounding regions indicated the reliability of the present reconstruction. A comparison of the reconstruction with Climate Research Unit (CRU) gridded data revealed that our reconstruction was representative of the NGS precipitation variability of a large region in the SETP.

Keywords: Tree rings; Non-growing season precipitation; Reconstruction; Southeastern Tibetan Plateau

1 Introduction

Unravelling the past climate often relies on proxy records. As a widely used proxy material, tree rings provide an opportunity to obtain long-term climate data (Fritts, 1976; Esper et al., 2002; D'Arrigo et al., 2005; Li et al., 2011; Büntgen et al., 2011, 2016; Cai et al., 2014; Yang et al., 2014; Schneider et al., 2015; Wilson et al., 2016; Keyimu et al., 2021). These long-term records enable us to identify the inter-annual, decadal and multi-decal variability of historical climatic conditions. They also provide a reference to better understand the nature of current climatic conditions (warming/cooling, drying/wetting) and to project the future regional climate, as well as the dynamic response of earth processes (e.g., forest growth, glacier retreat/advance, stream flow, drought frequency, and forest fires) to climate change.

Being the "third pole" of the Earth, the Tibetan Plateau (TP) (average 4000 m a.s.l.) is particularly sensitive to climate change and is one of the fastest warming places in the world (Chen et al., 2020). The average decadal temperature increase at the TP is 0.33°C, which is higher than the world's average decadal temperature increase of 0.20°C (Yan and Liu, 2014). Because of its geographical extent and position within the global circulation system, the TP plays a key role in regional and global atmospheric circulation patterns (Griessinger et al., 2017), not only affecting the mid-latitude westerlies, but also influencing the Asian monsoon circulation through its thermo-dynamical feedbacks (Duan et al., 2006; Rangwala, 2009; Wu et al., 2015).

There are large areas of coniferous forest distributed at high altitudes in the southeastern Tibetan Plateau (SETP). Due to their age and relative lack of disturbance they are a source of proxy material (tree rings) that can be used to reveal the past climatic conditions in this region (Bräuning and Mantwill, 2004; Fan et al., 2009; Fang et al., 2010; Li et al., 2011; Wang et al., 2015; Li and Li., 2017; Shi et al., 2017; Huang et al., 2019; Shi et al., 2019; Keyimu et al., 2021). Many dendroclimatological reconstructions of hydroclimatic variables have also been conducted in the SETP (Fan et al., 2008; Zhang et al., 2015; Wernicke et al., 2015; Griessinger et al., 2017; Li et al., 2017; He et al., 2018). However, few studies have focused on the reconstruction of precipitation history (He et al., 2012; Wernicke et al., 2015). The non-growing season (NGS) of vegetation (from November of the previous year to February of the current year) includes the non-monsoon and pre-monsoon seasons in the SETP, and water availability during the NGS might therefore have a constraining effect on radial tree growth (Linderholm and Chen, 2005). It is important to understand the long-term precipitation variations during the NGS to evaluate the current trend of precipitation variation and estimate its future patterns, and to determine the future responses of the forest ecosystem under the changing precipitation trend. To our knowledge, however, there have been no reports of the reconstruction of NGS precipitation in this area. This hinders our understanding of NGS variability from a long-term perspective.

In this study, we collected tree-ring cores of forest hemlock from the Xinzhu Village of northwestern Yunnan in the SETP. The main objectives of the present study were to (1) identify the relationship between the radial growth of forest hemlock and climate, (2) reconstruct the regional precipitation history, and (3) validate the reliability of the reconstruction. Our results not only improve the historical precipitation information available in the SETP, but also provide the basis to evaluate the current trend of regional NGS precipitation variation, as well as the future development of regional forest growth.

2 Materials and methods

2.1 Study area and sampling sites

Tree-ring core samples were collected from Xinzhu Village in Lijiang County in northwestern Yunnan. The sample site was in the Hengduan Mountains in the SETP (Fig. 1). The climate of the study area is regulated by a westerly circulation and the monsoon circulations of the Indian and Pacific oceans. “Hengduan” means “transverse” in the Chinese language, which implies that the mountains in this region lie in the transverse direction from south to north, and the area is a passageway for the Indian monsoon to flow in and climb up to the TP and other parts of the mainland. The SETP is susceptible to monsoon flow and atmospheric circulations (Bräuning and Mantwill, 2004). According to the Weixi meteorological station of the China Meteorological Administration, which was the closest station to our sampling site, the mean annual precipitation was 953 mm from 1955 to 2016. Most of the annual precipitation (Nearly 70%) concentrated in the monsoon season from May to October in this region (Fig. 2), and thus, tree growth is usually constrained by water availability during non-growing season. The coldest temperature was -2.9°C in January and the warmest temperature was 18.6°C in July. Tree-ring cores of forest hemlock were collected at a site that had not been impacted by anthropogenic disturbances. The elevation of the sampling site was 2,966 m a.s.l. A total of 48 tree-ring cores were extracted from 48 trees using a 5.1 mm diameter increment borer. We have used one sampling per tree method to improve the spatial representativity of radial tree growth. Sampling was conducted along an axis perpendicular to the slope inclination to avoid the impact of tension wood (Keyimu et al., 2020).

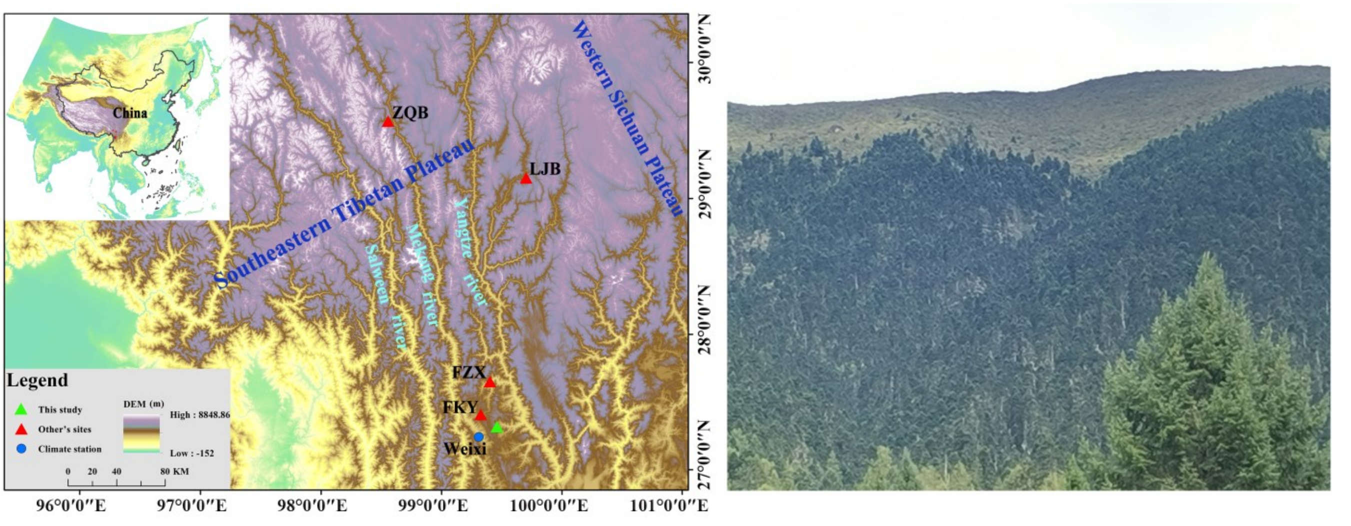

Figure 1: Map of the study area. The green triangle is the study site. The red triangles are the sites in other studies (previous year May – current year April PDSI reconstruction site in Fang et al., 2010; current year March – May PDSI reconstruction site in Fan et al., 2008; current year April – June PDSI reconstruction site in Li et al., 2017; current year May – June PDSI reconstruction site in Zhang et al., 2015). The blue dot is the meteorological station in Weixi County. On the right is the landscape image of tree ring sampling site.

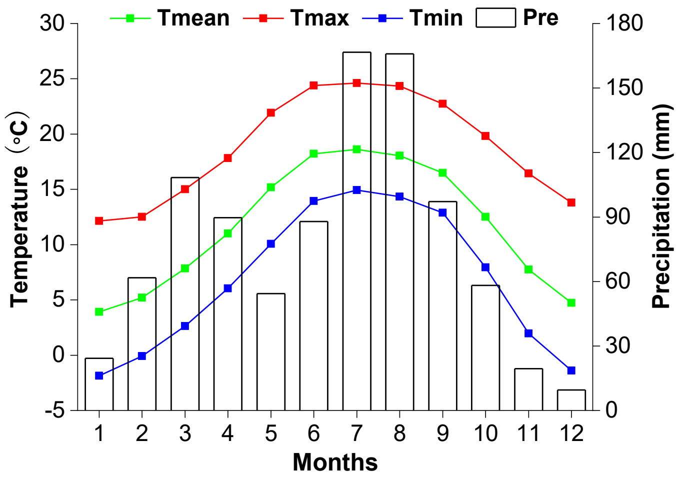

Figure 2: The ombrothermic diagram of the climate variables in the study area

2.2 Establishment of the tree-ring chronology

The tree-ring samples were treated with standard dendrochronological procedures. They were first glued onto wooden holders and air-dried, and then polished to a flat surface with sand paper until the tree rings were clearly visible. The LINTAB 6.0 tree ring measurement system was used to measure the tree-ring width (TRW). Crossdating was conducted visually by marking each sample at each ten-year interval, and then its quality was confirmed using the COFFECHA program (Holmes, 1983). Thirty-eight of the tree-ring cores were adopted for a further analysis after excluding the bad quality samples and the un-crossdated samples. The tree-ring series was detrended with a negative exponential model to remove the age dependency of tree growth (Cook et al., 1995). We have used the residual chronology since it removes the auto-correlation in tree ring growth and captures high frequent climate signal. The “dplR” software toolkit (Bunn, 2018) within the R software environment (R Core Team 2020) was used for detrending and chronology establishment. The reliable period of the chronology was determined based on the criterion of expressed population signal (EPS) > 0.85 (Wigley, 1984).

2.3 Climate data

Temperature and precipitation records were obtained from the Weixi meteorological station (27.17° N, 99.28° E, 2326 m a.s.l.) operated by the China Meteorological Administration. Data was available for the period of 1955–2005. Climate data (including the maximum, minimum and average temperatures, and precipitation) were provided by the China Meteorological Data Sharing Service Platform. A self-calibrated Palmer Drought Severity Index (scPDSI) was downloaded from the 3.26e gridded dataset of the Climate Research Unit (CRU) via the Royal Netherlands Meteorological Institute (KNMI) climate explorer (data accessed on 23rd December, 2020, data re-accessed for the updated version (CRU scPDSI 4.05 early) of PDSI data on 20th of April, 2021) using the coordinates of the tree ring sampling site. The range of CRU grid box is 27.0 – 27.5° N, 99.0 – 99.5° E.

2.4 Tree growth and climate relationship analysis

We analysed the relationship between climate and tree growth using Dendroclim 2002 software (Biondi and Waikul, 2004). Pearson correlation values and response function values were calculated for the relationships between TRW indices and climate variables for the period of 1955–2005. Due to the carry over effect of the climatic conditions of the previous-year on the current year tree growth (Fritts, 1976), the tree growth – climate relationship analysis spanned a 16-month period from June of the previous year to September of the current year. We also used the seasonalised climate variables because it made more eco-physiological sense for growth than single months. To observe the temporal stability of the climate influence on radial tree growth, we conducted a moving correlation analysis at a moving interval of 32 years. All the correlation results were considered significant at the 95% confidence level.

2.5 Climate reconstruction

According to the analysis of the relationship between the TRW indices and constraining climatic factors, we developed a linear regression model (Cook and Kairiukstis, 1990) for the climate reconstruction. As in many other tree ring based climate reconstructions, we tested the goodness-of-fit of the model using the leave-one-out cross-validation method (Michaelsen, 1987). We used the Pearson's correlation coefficient (r), explained variance (R^2), adjusted explained variance (R_{adj}^2), reduction of error (RE), sign test (ST), coefficient of efficiency (CE), and product mean test (Pmt) to evaluate the fidelity of the reconstruction model (Fritts et al., 1990).

3. Results

3.1 Characteristics of the TRW chronology

Residual TRW chronology of forest hemlock from the investigation area was established (Fig. 3). The descriptive statistics of the chronology were presented in Table 1. According to the criteria of EPS > 0.85, the most reliable length of the TRW chronology was 406 years (A.D. 1600–2005). The mean correlation among tree-ring series (Rbar) was 0.48, and the variance in the first eigenvector (VFE) was 27 %, which implied a relatively strong common signal among individual trees constituting the chronology. The relatively low inter-annual variability of the chronology was expressed by the small mean sensitivity value (0.23). The EPS and SNR values (average EPS and SNR were 0.89 and 6.87 for the total length chronology, respectively) further implied the existence of the common signal among each individual measurement series. In general, all the statistical parameters indicated the potential climate signal imprinted in our TRW chronology.

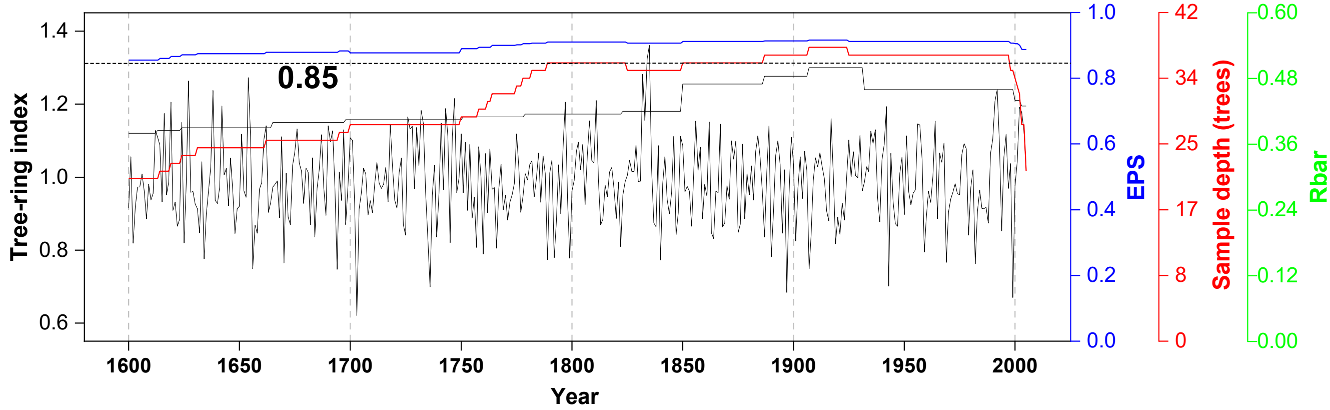

Figure 3: Plot of tree-ring residual chronology, the running inter-correlations among cores (Rbar, the green line), expressed population signal (EPS, the blue line) and the sample size (the red line). The Rbar and EPS were calculated using a 30-year window, with a 15-year lag. The horizontal dashed line denotes the EPS threshold level (0.85).

Table 1. Site information, chronology statistics and results of a common interval span analysis of residual tree-ring width (TRW) chronology from the Xinzhu Village, northwestern Yunnan in China

Type	Location	Elevation (m)	Time length	Number of cores	SD	MS	Rbar	SNR	EPS	VFE
Tree ring	99.43°E, 27.25°N	2966	1600–2005	38	0.22	0.23	0.48	6.87	0.89	0.27

Note: SD: standard deviation, MS: mean sensitivity, Rbar: mean inter-series correlation, SNR: signal-to-noise ratio, EPS: Expressed Population Signal, VFE: Variance in first eigenvector.

3.2 Tree growth and climate relationship analysis

According to the results of the tree growth and climate relationship analyses (Fig. 4), the precipitation during the NGS was the most important constraining factor ($R = 0.56$, $p < 0.001$) on the radial growth of forest hemlock in the study area. The results of a response function analysis further confirmed the strong correlation between NGS precipitation and forest hemlock radial growth. The results of a moving correlation analyses between TRW chronology and instrumental NGS precipitation record (Fig. 5) were positively significant (at 99%) during the investigated period (1956-2005), indicating that the NGS precipitation influence was stationary over time.

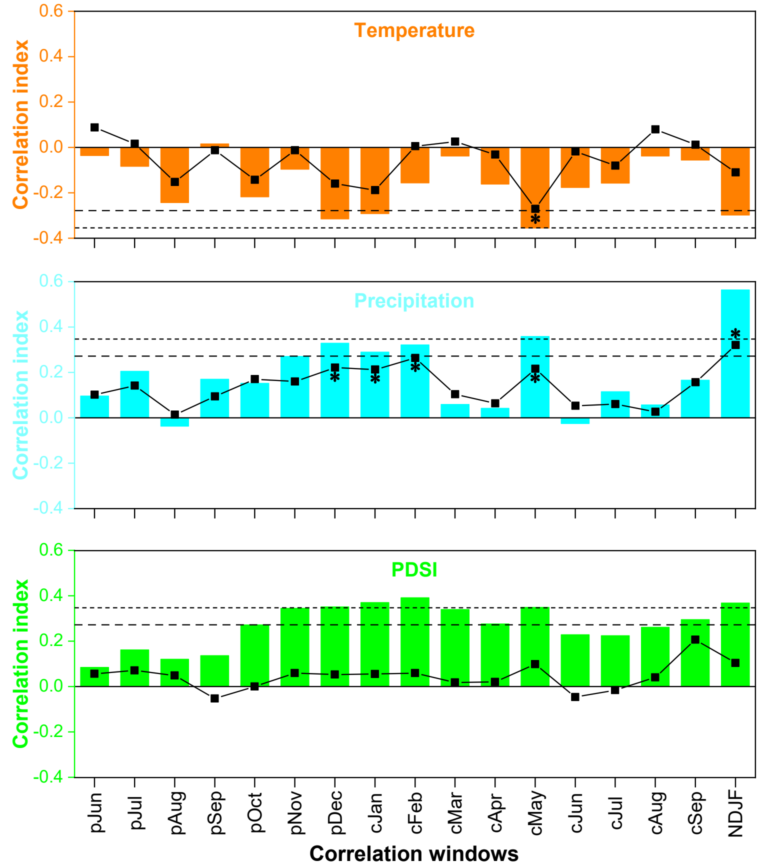

Figure 4: Correlations between tree-ring indices and temperature, precipitation, and scPDSI in the correlation windows from previous year June to current year September, as well as in NDJF (non-growing season, NGS) for the common period from 1956 to 2005. The horizontal dashed and dotted lines indicate the threshold of the correlations at the 95% and 99% significance levels. Black line with squares denotes the results of response function analysis between tree-ring indices and climate variables. The asterisks next to the squares denote the significant effects ($p < 0.05$) of response function analyses.

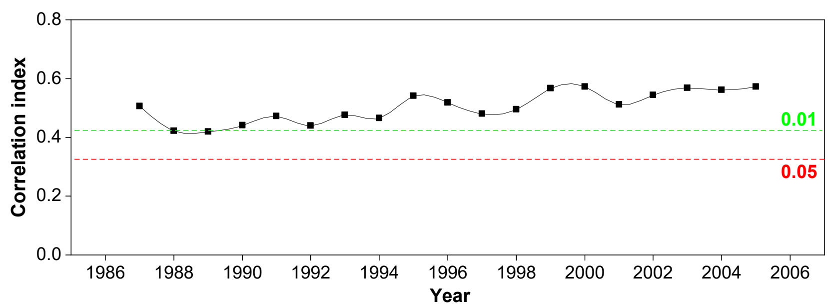

Figure 5: The moving correlation result between tree-ring width (TRW) chronology and non-growing season (NGS) precipitation during the period of 1956–2005. The horizontal red and green dashed lines denote the significance levels of 0.05 and 0.01, respectively.

3.3 Non-growing season precipitation reconstruction

According to the relationship between the TRW chronology and NGS precipitation, we developed a linear regression model (y = 229.94x-109.45 mm) and reconstructed the historical NGS precipitation series, which extended back to A.D. 1600 (Fig. 6a). In the model, y is the NGS precipitation, and x is the TRW index. The reconstruction accounted for 28.5% of the instrumental NGS precipitation variability during the common time span (1956–2005). Figure 6b shows the similarities between the instrumental and reconstructed NGS precipitation series. We used a leave-one-out cross-verification method to evaluate the legitimacy of the reconstruction model (Table 2). The positive RE and CE values (0.18 and 0.15, respectively) were indicative of legitimacy of the reconstruction. The significant value (at 95%) of sign test implied that the model predicted values were generally in line with the variation trend of instrumental values. In addition, the significant values of F test (at 99%) and PM test (at 95%) further confirmed the validity of the reconstruction. Overall, the statistics indicated that the reconstruction model possessed good predictive skills.

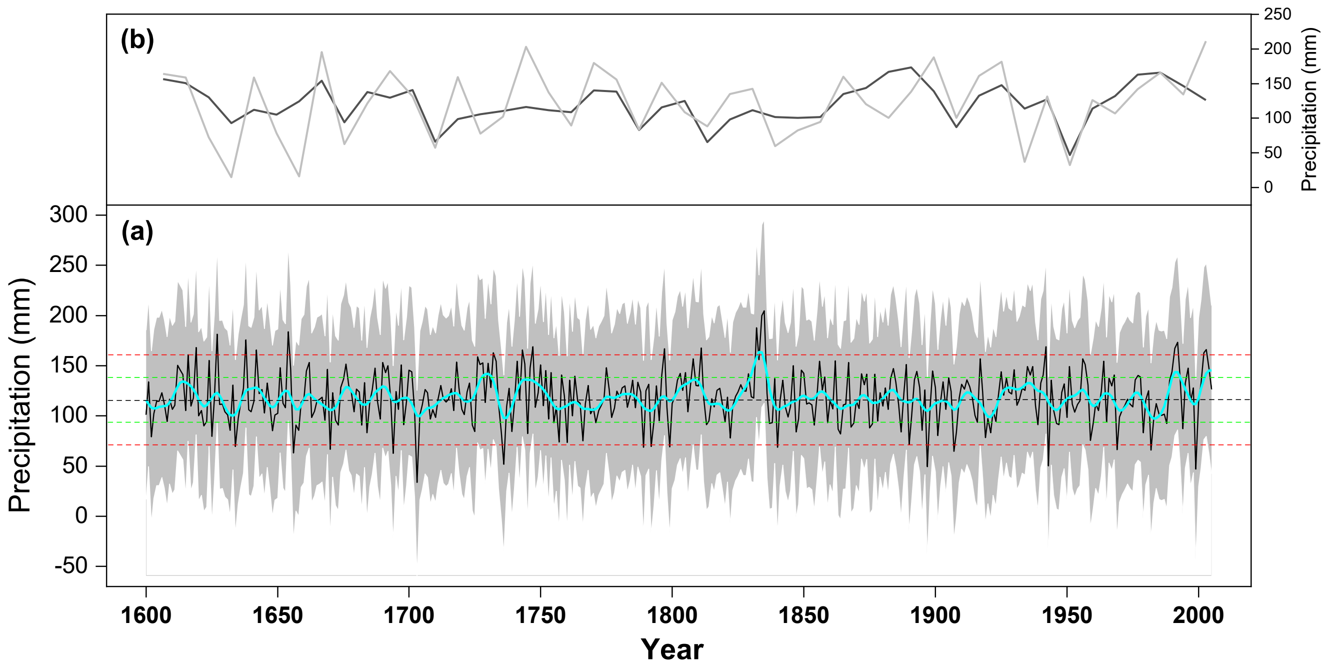

Figure 6: Non-growing season (NGS) precipitation reconstruction from A.D. 1600 to 2005. (a) The black line is the reconstruction series, the thick cyan line is the 11- year loess smoothed series. The horizontal black dashed line is the mean of NGS precipitation value during from A.D. 1600–2005. The horizontal green and red dashed lines are the one time and two

times the of standard deviations of NGS precipitation, which demonstrated the boundaries of dry and extremely dry (below mean), and wet and extreme wet (above mean) years. The grey shading indicated the 95% confidence interval of the reconstruction; (b) Instrumental (black) and reconstructed (grey) NGS precipitation during their common period of 1956–2005.

Table 2. Leave-one-out verification statistics for the non-growing season (NGS) precipitation reconstruction

	R	R^2	R_{adj}^2	*F*	Sign-test	*Pmt*	*RE*	*CE*
Calibration	0.561	0.315	0.285	–	–	–	–	–
Verification	0.524	0.274	0.235	18.6**	36+/13–*	7.89*	0.18	0.15

Note: *R* correlation coefficient, R^2 explained variance, R_{adj}^2 is the adjusted explained variance, *F* *F*-test, Sign-test sign of paired observed and estimated departures from their mean on the basis of the number of agreements/disagreements, Pmt product mean test, RE reduction of error, CE coefficient of efficiency. * $p < 0.05$, ** $p < 0.01$

3.4 Characteristics of the NGS precipitation reconstruction

Figure 6a shows the reconstructed NGS precipitation over the past 406 years (A.D. 1600–2005). The mean of the reconstructed NGS precipitation series was 117.87 mm, and the standard deviation (SD) was 25.64 mm. We pre-defined the years that had NGS precipitation below 92.23 mm (mean–SD) as dry NGS years, and below 66.59 mm (mean–2SD) as extremely dry years, whereas we defined years that had precipitation above 143.51 mm (mean+SD) as wet NGS years, and above 169.15 mm (mean+2SD) as extremely wet NGS years. Accordingly, the NGS was extremely dry during the years A.D. 1656, 1670, 1694, 1703, 1736, 1897, 1907, 1943, 1969, 1982, and 1999. In contrast, the NGS was extremely wet during the years A.D. 1627, 1638, 1654, 1832, 1834–1835, and 1992. The dry/wet periods and some of the extreme dry/wet NGS periods in the present reconstruction were synchronised with dry/wet periods and extreme dry/wet periods in previously reported PDSI reconstruction from the surrounding region (Fig. 7, Table S2, Table S3), though some dissimilarities were also existed. As shown in Fig. 8, the instrumental (**a**) and reconstructed (**b**) NGS precipitation series could represent the climatic conditions over a similar area in the SETP.

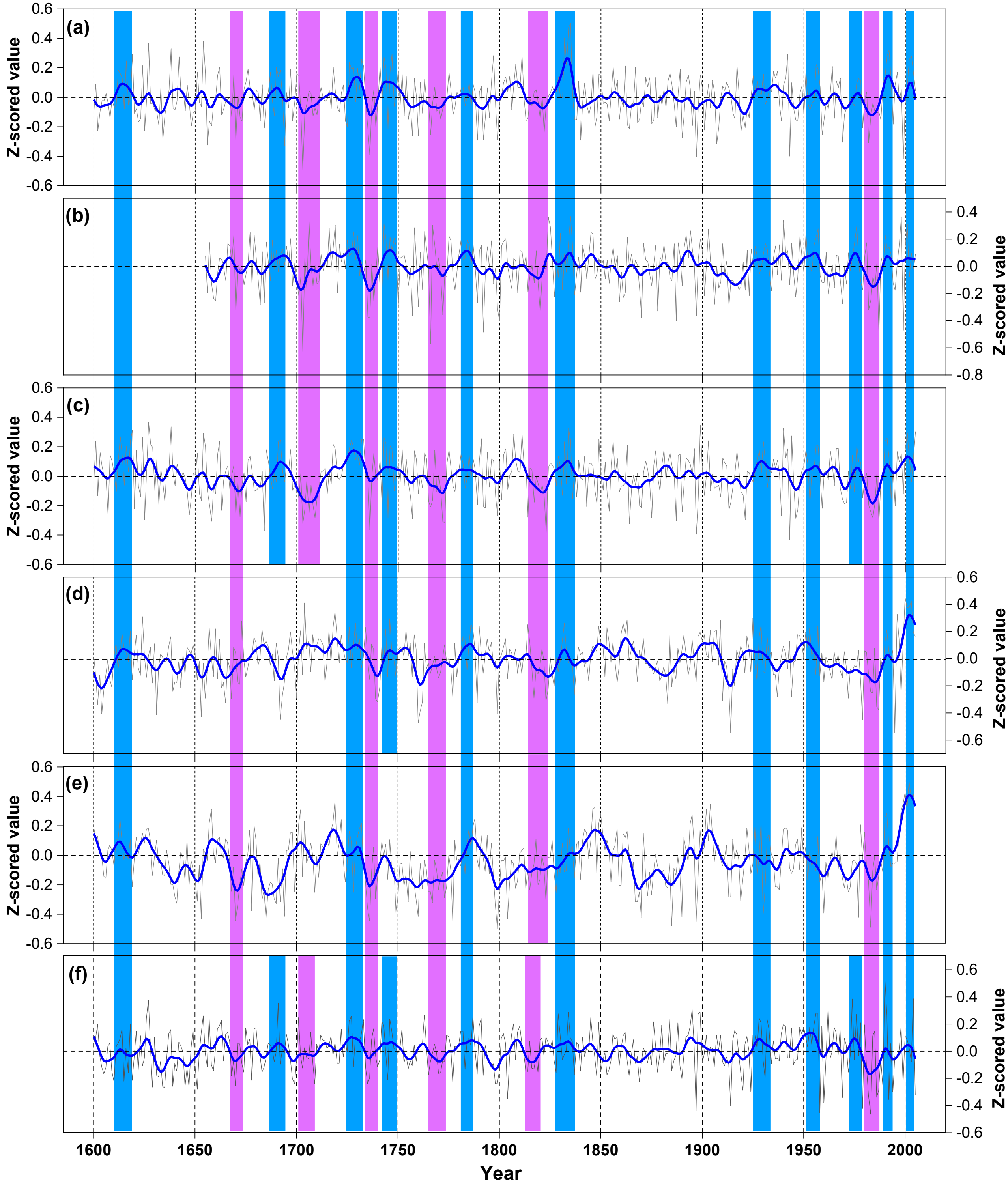
(a)
(b)
(c)
(d)
(e)
(f)
Z-scored value
Year
1600
1650
1700
1750
1800
1850
1900
1950
2000

190

Figure 7: Comparisons of the hydroclimatic reconstructions in different studies. (a) The non-growing season (NGS) precipitation reconstruction in the present study. (b) The current year March – May average Palmer Drought Severity Index (PDSI) reconstruction in Fan et al. (2008). (c) The reconstruction of average PDSI from May of the previous year to April of the current year in Fang et al. (2010). (d) The current year May-June average PDSI reconstruction in Zhang et al. (2015). (e) The current year April-June average PDSI reconstruction in Li et al. (2017). (f) drought series extracted from Asian Monsoon Atlas from the nearest point (Cook et al. 2010). The blue and purple bars show the common wet and dry periods of the different reconstructions, respectively.

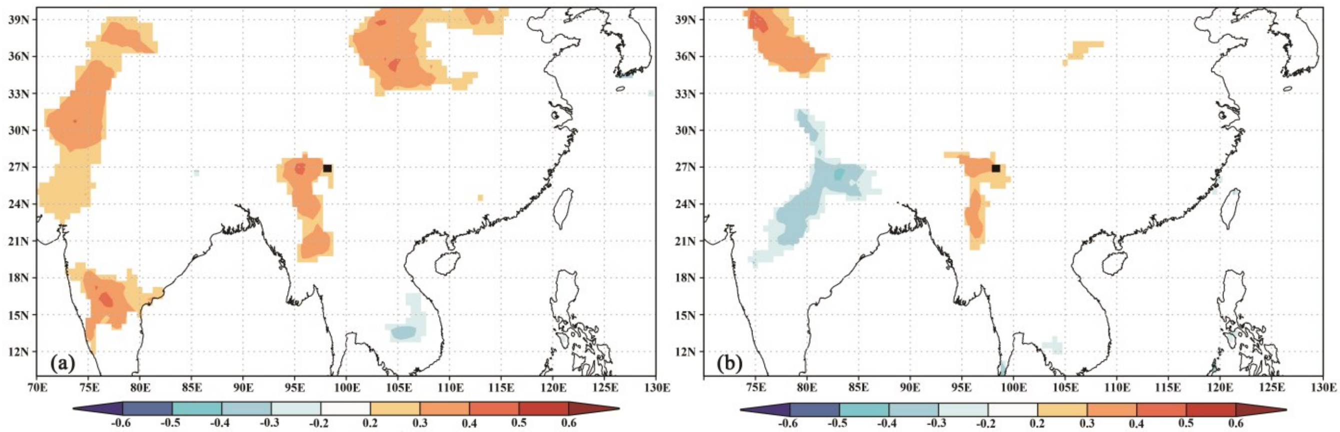

Figure 8: Spatial correlations between the actual (a) and reconstructed (b) non-growing season (NGS) precipitation and a gridded dataset of the NGS precipitation (average from November of the previous year to February of the current year) during their overlapping periods (1956–2005). The black square indicates the location of the study site.

4. Discussion

4.1 Tree growth and climate relationship

The results of the tree growth and climate relationship analyses suggested that the forest hemlock radial growth in the northwestern Yunnan region of the SETP was strongly constrained by hydroclimatic factors. According to the Pearson correlation analysis, the influence of precipitation during the NGS on radial tree growth was greater than that of any other investigated climate variables and any correlation window. The response function analysis further confirmed the strong impact of NGS precipitation. In addition, the results of 32-year interval of moving correlation analysis (Fig. 5) suggested the temporally consistent influence of NGS precipitation on forest hemlock radial growth in this region. The importance of NGS precipitation on the radial tree growth could be attributed to the fact that precipitation during the NGS compensated for the soil moisture, which was crucially important for supporting tree growth in the following season (Linderholm and Chen, 2005; Treydte et al. 2006; Wu et al., 2019; Li et al., 2021). This is because tree growth is often water stressed in the early stages of its growth in each year on the SETP when the monsoon precipitation does not arrive (Bräuning and Mantwill, 2004; Zhang et al., 2015), and the earlywood of tree rings mainly use spring melt water (Zhu et al., 2021). The eco-physiological importance of NGS precipitation on tree growth and tree water usage was also revealed by isotope ratios method-based investigations. Brinkmann et al's (2018) study showed that nearly 40% of the uptaken water by *Fagus sylvatica* and *Picea abies* trees in a temperate forest of middle Europe are sourced from NGS precipitation. Tree-ring oxygen isotope ratios ($\delta^{18}O$) are demonstrated to contain NGS precipitation signals in the Himalayan region (Huang et al., 2019; Zhu et al., 2021). Huang et al's (2019) study revealed that NGS precipitation (snowfall) increased the snow-depth and the later snowmelt compensated soil moisture in the spring and early summer, which was a crucially important water source for the Juniper growth in the southwestern Tibetan Plateau. Zhu et al's (2021) investigation in the western Himalaya revealed that formation of earlywood in tree rings of *Pinus wallachina* depended on the snowmelt originated from NGS precipitation. The weak influence of precipitation on regional forest hemlock growth during March and April and strong influence during May was connected with the saddle-shaped monthly rainfall pattern of this area (Fig. 2). The correlations between precipitation and the TRW chronology were not significant during the growing season (June-September) because an adequate water supply was available in the monsoon season.

Precipitation during the NGS over the SETP falls as snow. According to Sommerfeld et al. (1993) and Stadler et al. (1996), the development of a snowpack insulates the underlying soil from freezing temperatures, which creates unfrozen soil conditions and most of the soil processes that are active during warmer conditions also persist under snow cover, albeit at a reduced rate (Edwards, 2007). Unfrozen soil can reduce the cold and frost damage to the shallow root systems of conifer trees in this region (Schenk and Jackson, 2002). A reduction in the cold damage to roots decreases the energy required to form new roots in the following growth year (Pederson et al., 2004), with the saved energy potentially used to initiate xylogenesis and form earlywood cells. Evergreen tree species are known to carry out year-round photosynthetic activity (Oquist and Huner, 2003; Prats and Brodersen, 2020), albeit at a slower rate during the NGS, and therefore, the higher moisture availability contributes to the carbohydrate and energy accumulation process of forest hemlock in the investigation area.

In contrast, the radial tree growth was negatively correlated to temperature in most correlation windows (Fig. 4). This can be explained by the fact that higher temperature enhances evapotranspiration, and thus decreases water availability, which eventually constrains tree growth. The negative impact of NGS temperature on radial tree growth was obvious because the strengthened evaporation due to higher temperatures might reduce the moisture compensation to the soil layer and cause water stress during the early stage of the following growth season.

4.2 Validity of the reconstructed precipitation series

We have tried to validate the fidelity of the newly reconstructed series from different aspects. Although we used the residual TRW chronology in the present study, which removes autocorrelation (Cook and Kairiukstis, 1990) to capture the high frequency climate signals as in Fan et al. (2008) and Chen et al. (2016), the variability of dry and wet NGS at different scales was still retained in our reconstructed series. The reconstructed series in the present study demonstrated the variation in dry and wet NGS years (Fig. 6a). As in many other proxy based historical climate reconstruction studies, we compared our NGS precipitation series with other hydroclimatic reconstructions from the surrounding areas to investigate the reliability of our reconstruction. There are only countable numbers of hydroclimatic (PDSI) reconstructions in the nearby region, and not any case of precipitation reconstruction. Hence, we could only compare the present NGS precipitation reconstruction with existing PDSI reconstructions (Fig. 7). The compared PDSI reconstructions are of spring or early summer, because drought climate during these seasons usually associated with the winter precipitation, it makes certain sense to carry out the comparative analysis. The correlation coefficients between our NGS precipitation reconstruction and the PDSI reconstructions of Fan et al. (2008), Fang et al. (2010), Zhang et al. (2015) and Li et al. (2017) were 0.51 (n = 702), 0.35 (n = 1062), 0.25 (n = 1062) and 0.22 (n = 1016) ($p < 0.001$). We have extracted the drought series of Asian Monsoon Atlas (Cook et al.2010) from the nearest point to our investigation site and compared it with the NGS precipitation reconstruction in present study ($R = 0.35$, n = 1062, $p < 0.001$). As can be observed from Fig. 7, there were dry and wet periods in compared reconstruction series which were consistent with the NGS precipitation variabilities. These similarities indicated the reliability of our NGS precipitation reconstruction to some extent. The correlation coefficients for the present reconstruction with those of Fan et al. (2008) and Fang et al. (2010) were greater than those with Li et al. (2017) and Zhang et al. (2015). These differences were probably due to the different distances among the study sites. Although, the major dry and wet periods were similar in the hydroclimatic reconstructions referenced above, there were still certain discrepancies in duration and the strength of the dry/wet climatic conditions. This is probably because of the differences in the types of hydroclimatic variables (precipitation, PDSI), specific seasons reconstructed (annual, seasonal), tree species (species with different drought tolerances), chronology recording methods (standard chronology, residual chronology), length of calibration period, sample replication and the geomorphic differences of the tree ring sampling sites (altitude, slope) (Table S1).

In addition, we uploaded both of the instrumental and reconstructed NGS precipitation data for the same period of 1956–2005 on the KNMI website and conducted a spatial correlation analyses with the CRU gridded climate dataset. The similar patterns of spatial correlation between the instrumental and reconstructed dataset (Fig. 8) indicated that the present reconstruction was reliable and could represent the NGS precipitation over a large area in the SETP. Besides, the occurrence of some historical great drought events in the Asian monsoon area (Cook et al., 2010, Kang et al., 2013), i.e., the 1756–1768 (strange parallels drought), 1790, 1792–1796 (east India drought) and 1920s (China mega-drought), matched the dry NGS periods in our reconstruction, which also further confirmed the reliability of our reconstruction.

5. Conclusion

In this study, we investigated 406 years of residual TRW chronology of forest hemlock in the SETP, China. The climate and tree growth relationship analyses showed that the TRW chronology was mostly negatively correlated with the thermal variable (temperature), whereas it was positively correlated with hydroclimatic variables (precipitation) and PDSI, indicating that hydroclimatic conditions determined the radial growth of forest hemlock in this region. Accordingly, we derived a linear model of the relationship between climate and tree growth, which accounted for 28.5% of the actual NGS precipitation variance (1956–2005), and we used the model to reconstruct the historical (A.D. 1600–2005) NGS precipitation. The reconstructed series showed that the NGS was extremely dry during the years A.D. 1656, 1670, 1694, 1703, 1736, 1897, 1907, 1943, 1969, 1982 and 1999. In contrast, the NGS was extremely wet during the years A.D. 1627, 1638, 1654, 1832, 1834–1835 and 1992. A comparison between the NGS precipitation reconstruction in this study and PDSI reconstructions from nearby regions revealed a coherency in the timing of dry and wet episodes, suggesting the reliability of our reconstruction.

Data availability. The climate reconstruction series in this study can be obtained from Zongshan Li after the paper publication.

Author contributions. ZSL and MK conceived the study; ZSL, ZXF, XCW collected the tree-ring data; MK, ZSL, ZXF, KYF, XCW elaborated the methodology; MK, ZSL, WLC analysed the data; MK, ZSL led the writing of the manuscript; ZSL and ZXF revised the manuscript; BJF and GHL validated the final manuscript.

Competing interests. The authors declare that they have no conflict of interest.

Acknowledgement. This work was funded by the National Key Research Development Program of China (2016YFC0502105), the second Tibetan Plateau Scientific Expedition and Research (STEP) Program (2019QZKK0502). We are grateful to the editor and anonymous reviewers for their valuable comments and suggestions to improve this article.

References

Biondi. F. and Waikul, K.: DENDROCLIM2002: a C++ program for statistical calibration of climate signals in tree ring chronologies, Comput. Geosci., 30(3), 303-311, https://doi.org/10.1016/j.cageo.2003.11.004, 2004

Bräuning, A. and Mantwill, B.: Summer temperature and summer monsoon history on the Tibetan Plateau during the last 400 years recorded by tree rings, Geophys. Res. Lett., 31, L24205, https://doi.org/10.1029/2004GL020793, 2004

Bunn, A. G. and Korpela, M.: An introduction to dplR. The Comprehensive R Archive Network, https://cran.biodisk.org/web/packages/dplR/vignettes/intro-dplR.pdf, 2018

Büntgen, U., Myglan, V. S., Ljungqvist, F. C., McCormick, M., Di Cosmo N., Sigl, M., Jungclaus, J., Wagner, S., Krusic, P. J., Esper, J., Kaplan, J. O., de Vaan MAC., Luterbacher, J., Wacker, L., Tegel, W. and Kirdyanov, A. V.: Cooling and societal change during the Late Antique Little Ice Age from 536 to around 660 AD, Nat. Geosci., 9, 231–236, https://doi.org/10.1038/ngeo2652, 2016

Büntgen, U., Tegel, W., Nicolussi, K., McCormick, M., Frank, D., Trouet, V., Kaplan, J. O., Herzig, F., Heussner, K. U., Wanner, H., Luterbacher, J. and Esper, J.: 2500 years of European climate variability and human susceptibility, Science, 331, 578–582, https://doi.org/10.1126/science.1197175, 2011

Cai, Q. F, Liu, Y., Lei, Y., Bao, G. and Sun, B.: Reconstruction of the march-august PDSI since 1703 AD based on tree rings of Chinese pine (*Pinus tabulaeformis* Carr.) in the Lingkong Mountain, southeast Chinese loess Plateau, Clim. Past., 10, 509–521, https://doi.org/10.5194/cp-10-509-2014, 2014

Chen, F., Yuan, Y. J, Zhang, T. W, Shang, H.: Precipitation reconstruction for the northwestern Chinese Altay since 1760 indicates the drought signals of the northern part of inner Asia, Int. J. Biometeorol., 60(3), 455-463. https://doi.org/10.1007/s00484-015-1043-5, 2016

Cook, E. R. and Kairiukstis, A.: Methods of Dendrochronology: Applications in the Environmental Sciences, Kluwer Academic Press, Dordrecht, 1990

Cook, E. R., Anchukaitis, K. J., Buckley, B. M., D'Arrigo, R. D., Jacoby, G. C. and Wright, W. E.: Asian monsoon failure and megadrought during the last millennium, Science, 328(5977), 486-489, https://doi.org/10.1126/science.1185188, 2010

Cook, E. R., Briffa, K. R., Meko, D. M., Graybill, D. A. and Funkhouser, G.: The 'segment length curse' in long tree-ring chronology development for palaeoclimatic studies, Holocene, 5(2), 229-237. https://doi.org/10.1177/095968369500500211, 1995

D'Arrigo, R. D., Mashig, E., Frank, D. C., Wilson, R. J. S. and Jacoby, G. C.: Temperature variability over the past millennium inferred from Northwestern Alaska tree rings, Clim. Dynam., 24, 227-236. https://doi.org/10.1007/s00382-004-0502-1, 2005

Duan, K., Yao, T. and Thompson, L.: Response of monsoon precipitation in the Himalayas to global warming, J. Geophys. Res., 111, D19110. https://doi.org/10.1029/2006JD007084, 2006

Edwards, A. C., Scalenghe, R., Freppaz, M.: Changes in the seasonal snow cover of alpine regions and its effect on soil processes: a review. Quat. Int., 162-163, 172-181. https://doi.org/10.1016/j.quaint.2006.10.027, 2007

Esper, J.: 1300 years of climatic history for Western Central Asia inferred from tree rings, Holocene, 12(3), 267-277. https://org.doi.10.1191/0959683602hl543rp, 2002

Fan, Z. X., Bräuing, A. and Cao, K. F.: Tree-ring based drought reconstruction in the central Hengduan Mountains region (China) since AD 1655, Int. J. Climatol., 28, 1879–1887, https://doi.org/10. 1002/joc.1689, 2008

Fan, Z. X., Bräuning, A., Yang, B. and Cao, K. F.: Tree ring density-based summer temperature reconstruction for the central Hengduan Mountains in southern China, Glob. Planet. Change, 65 (1-2), 1-11. https://doi.org/10.1016/j.gloplacha.2008.10.001, 2009

Fang, K. Y, Gou, X. H, Chen, F., Li, J. B., D'Arrigo, R., Cook, E. D, Yang, T. and Davi, N.: Reconstructed droughts for the southeastern Tibetan Plateau over the past 568 years and its linkages to the Pacific and Atlantic Ocean climate variability, Clim. Dyn., 35(4), 577–585. https://doi.org/10.1007/s00382-009-0636-2, 2010

Fritts, H. C., Guiot, J. and Gordon, G. A.: Verification. In: Cook E and Kairiukstis LA, eds., Methods of Dendrochronology: Applications in the Environmental Sciences. Dordrecht, Kluwer Academic Publishers, 178-184, 1990

Fritts, H. C.: Tree rings and climate. Academic Press, London, 1976

Griessinger, J., Bräuning, A., Helle, G., Hochreuther, P. and Schleser, G.: Late Holocene relative humidity history on the southeastern Tibetan plateau inferred from a tree ring $\delta^{18}O$ record: recent decrease and conditions during the last 1500 years, Quat. Int., 430, 52–59, http://dx.doi.org/10.1016/j.quaint.2016.02.011, 2017

He, H. M., Bräuning, A., Griessinger, J., Hochreuther, P. and Wernicke, J.: May–June drought reconstruction over the past 821 years on the southcentral Tibetan Plateau derived from tree-ring width series, Dendrochronologia, 47, 48–57, https://doi.org/10.1016/j.dendro.2017.12.006, 2018

He, H. M., Yang, B., Bräuning, A., Wang, J. L. and Wang, Z. Y.: Tree-ring derived millennial precipitation record for the south-central Tibetan plateau and its possible driving mechanism, Holocene, 23 (1), 36-45, https://doi.org/10.1177/0959683612450198, 2012

Holmes, R. L.: Computer-assisted quality control in tree-ring dating and measurement, Tree-ring Bulletin, 43, 69-75, 1983

Huang, R., Zhu, H. F., Liang, E. Y., Liu, B., Shi, J. F., Zhang, R. B., Yuan, Y. J., Griessinger, J.: A tree ring-based winter temperature reconstruction for the southeastern Tibetan Plateau since 1340 CE, Clim. Dyn., 53, 3221-3233. https://doi.org/10.1007/s00382-019-04695-3, 2019

Kang, S. Y, Bao, Y., Qin, C., Wang, J. L, Feng, S., Liu, J. J.: Extreme drought events in the years 1877–1878, and 1928, in the southeast Qilian mountains and the air–sea coupling system. Quat. Int., 283(427), 85-92. https://doi.org/10.1016/j.quaint.2012.03.011, 2013

Keyimu, M., Li, Z. S., Liu, G. H., Fu, B. J., Fan, Z. X., Wang, X. C. Zhang, Y. D., Halik, U.: Tree-ring based minimum temperature reconstruction on the southeastern Tibetan Plateau, Quat. Sci. Rev., 251, 106712. https://doi.org/10.1016/j.quascirev.2020.106712, 2021

Keyimu, M., Wei, J. S., Zhang, Y. X., Zhang, S., Li, Z. S., Ma, K. M., Fu, B. J.: Climate signal shift under the influence of prevailing climate warming – Evidence from *Quercus liaotungensis* on Dongling Mountain, Beijing, China, Dendrochronologia, 60, 125683. https://doi.org/10.1016/j.dendro.2020.125683, 2020

Li, J. B., Shi, J. F., Zhang, D. D., Yang, B., Fang, K. Y. and Yue, P. H.: Moisture increase in response to high-altitude warming evidenced by tree-rings on the southeastern Tibetan Plateau, Clim. Dyn., 48, 649–660. https://doi.org/10.1007/s00382-016-3101-z, 2017

Li, T., Li, J.B.: A 564-year annual minimum temperature reconstruction for the east central Tibetan Plateau from tree rings, Glob. Planet. Change, 157, 165-173. https://doi.org/10.1016/j.gloplacha.2017.08.018, 2017.

Li, Z. S., Zhang, Q. B. and Ma, K. P.: Tree-ring reconstruction of summer temperature for A.D. 1475–2003 in the central Hengduan Mountains, northwestern Yunnan, China, Clim. Change, 110(1-2), 455-467, https://doi.org/10.1007/s10584-011-0111-z, 2011

Linderholm, H. W., Chen, D.: Central Scandinavian winter precipitation variability during the past five centuries reconstructed from *Pinus sylvestris* tree rings, Boreas, 34, 43–52, https://doi.org/10.1080/03009480510012845, 2005

Michaelsen, J.: Crossevalidation in statistical climate forecast models, J Clim. App. Meteorol., 26, 1589-1600, 1987

R: A language and environment for statistical computing. R Foundation for Statistical Computing, Vienna, Austria. URL https://www.R-project.org/., 2020

Oquist, G., Huner, N. P.: Photosynthesis of overwintering evergreen plants, Annu. Rev. Plant Biol., 54, 329–355. https://doi.org/10.1146/annurev.arplant.54.072402.115741, 2003

Prats, K. A., Brodersen, C. R.: Seasonal coordination of leaf hydraulics and gas exchange in a wintergreen fern, AoB Plants, 12(6), 1–13. https://doi.org/10.1093/aobpla/plaa048, 2020

Pederson, N., Cook, E. R., Jacoby, G. C., Peteet, D. M., Griffin, K. L.: The influence of winter temperatures on the annual radial growth of six northern range margin tree species, Dendrochronologia, 22 (1), 7–29. https://doi.org/10.1016/j.dendro.2004.09.005, 2004

Rangwala, I., Miller, J. R. and Xu, M.: Warming in the Tibetan Plateau: Possible influences of the changes in surface water vapor, Geophys. Res. Lett., 36, L06703, https://doi.org/10.1029/2009GL037245, 2009

Schenk, H. J., & Jackson, R. B.: The global biogeography of roots. Ecol. Monogr., 72, 311–328. https://doi.org/10.1890/0012-9615(2002)072[0311:TGBOR]2.0.CO;2, 2002

Schneider, L., Smerdon, J. E., Büntgen, U., Wilson, R. J. S., Myglan, V. S., Kirdyanov, A. V. and Esper, J.: Revising mid-latitude summer temperatures back to AD 600 based on a wood density network, Geophys. Res. Lett., 42, 4556-4562. https://doi.org/10.1002/2015GL063956, 2015

Shi, C. M., Sun, C., Wu, G. C., Wu, X. C., Chen, D. L., Masson-Delmotte, V., Li, J. P., Xue, J. Q., Li, Z. S., Ji, D. Y., Zhang, J., Fan, Z. X., Shen, M. G., Shu, L. F., Ciais, P.: Summer temperature over Tibetan Plateau modulated by Atlantic multi-decadal variability, J. Clim., 32, 4055-4067. https://doi.org/10.1175/JCLI-D-17-0858.1, 2019

Shi, S. Y., Li, J. B., Shi, J. F., Zhao, Y. S. and Huang, G.: Three centuries of winter temperature change on the southeastern Tibetan plateau and its relationship with the Atlantic Multidecadal Oscillation, Clim. Dyn., 49, 1305-1319. https://doi.org/10.1007/s00382-016-3381-3, 2017

Sommerfeld, R. A., Mosier, A. R., Musselman, R. C.: CO_2, CH_4 and N_2O flux through a Wyoming snowpack and implications for global budget, Nature, 361, 140–142, https://doi.org/10.1038/361140a0, 1993

Stadler, D., Wunderli, H., Auckenthaler, A., Fluhler, H.: Measurement of frost induced snowmelt runoff in a forest soil, Hydrol. Process., 10, 1293–1304, https://doi.org/10.1002/(SICI)1099-1085(199610)10:10<1293::AID-HYP461>3.0.CO;2-I, 1996

Wang, J. L., Yang, B., Ljungqvist, F. C.: A millennial summer temperature reconstruction for the eastern Tibetan Plateau from tree-ring width, J. Clim., 28(13), 5289-5304. https://doi.org/10.1175/JCLI-D-14-00738.1, 2015

Wernicke, J., Griessinger, J., Hochreuther, P., Bräuning, A.: Variability of summer humidity during the past 800 years on the eastern Tibetan plateau inferred from $\delta^{18}O$ of tree-ring cellulose. Clim. Past, 10(4), 3327-3356. https://doi.org/10.5194/cp-11-327-2015. 2015

Wigley, T. M., Briffa, K. R., and Jones, P. D.: On the average value of correlated time series, with applications in dendroclimatology and hydrometeorology, J. Clim. Appl. Meteorol., 23, 201–213, https://doi.org/10.1175/1520-0450(1984)0232.0.CO;2, 1984

Wilson, R., Anchukaitis, K., Briffa, K. R., Büntgen, U., Cook, E., D'Arrigo, R., Davi, N., Esper, J., Frank, D., Gunnarson, B., Hegerl, G., Helama, S., Klesse, S., Krusic, P.J., Linderholm, H.W., Myglan, V., Osborn, T.J., Rydval, M., Schneider, L., Schurer, A., Wiles, G., Zhang, P. and Zorita, E.: Last millennium northern hemisphere summer temperatures from tree rings: Part I: the long-term context, Quat. Sci. Rev., 134, 1-18. https://doi.org/10.1016/j.quascirev.2015.12.00, 2016

Wu, G., Duan, A., Liu, Y., Mao, J., Ren, R., Bao, Q., He, B., Liu, B. and Hu, W.: Tibetan Plateau climate dynamics: recent research progress and outlook, Natl. Sci. Rev., 2, 100–116, https://doi.org/10.1093/nsr/nwu045, 2015

Wu, X. C., Li, X. Y., Liu, H. Y., Ciais, P., Li, Y. Q., Xu, C. Y., Babst, F., Guo, W. C., Hao, B. Y., Wang, P., Huang, Y. M., Liu, S. M., Tian, Y. H., He, B. and Zhang, C. C.: Uneven winter snow influence on tree growth across temperate China, Glob. Change Biol., 25, 144–154. https://doi.org/10.1111/gcb.14464, 2019

Yan, L. and Liu, X.: Has climatic warming over the Tibetan Plateau paused or continued in recent years? J. Earth Ocean Atmos. Sci., 1, 13–28, 2014

Yang, B., Qin, C., Wang, J., He, M., Melvin, T. M., Osborn, T. J.: A 3,500-year tree-ring record of annual precipitation on the northeastern Tibetan Plateau, Proc. Natl. Acad. Sci. U. S. A., 111(8), 2903-2908. https://doi.org/10.1073/pnas.1319238111, 2014

Zhang, Q. B., Evans, M. N., Lyu, L. X.: Moisture dipole over the Tibetan Plateau during the past five and a half centuries, Nat. Commun., 6, 8062. https://doi.org/10.1038/ncomms9062, 2015

Zhu, H. F., Huang, R., Asad, F., Liang, E. Y., Bräuning, A., Zhang, X. Z., Dawadi, B., Man, W. M., Griessinger, J.: Unexpected climate variability inferred from a 380-year tree-ring earlywood oxygen isotope record in the Karakoram, Northern Pakistan, Clim. Dyn., https://doi.org/10.1007/s00382-021-05736-6, 2021